JGR Oceans

RESEARCH ARTICLE
10.1029/2024JC021716

Compound Minor Floods and the Role of Discharge in the Delaware River Estuary

Kelly McKeon[1,2] **and Christopher G. Piecuch**[1]

[1]Woods Hole Oceanographic Institution, Woods Hole, MA, USA, [2]MIT-WHOI Joint Program in Oceanography/Applied Ocean Sciences & Engineering, Cambridge, MA, USA

Key Points:

- Most minor floods observed by tide gauges in the Delaware River Estuary are compound minor floods
- River discharge plays an important role in the magnitude and frequency of minor floods
- Open-ocean effects and river discharge effects make similar contributions to minor flooding in the upper estuary

Supporting Information:

Supporting Information may be found in the online version of this article.

Correspondence to:

K. McKeon,
kmckeon@whoi.edu

Citation:

McKeon, K., & Piecuch, C. G. (2025). Compound minor floods and the role of discharge in the Delaware River Estuary. *Journal of Geophysical Research: Oceans*, *130*, e2024JC021716. https://doi.org/10.1029/2024JC021716

Received 13 AUG 2024
Accepted 13 FEB 2025

Author Contributions:

Conceptualization: Kelly McKeon, Christopher G. Piecuch
Formal analysis: Kelly McKeon
Funding acquisition: Christopher G. Piecuch
Methodology: Kelly McKeon, Christopher G. Piecuch
Resources: Christopher G. Piecuch
Supervision: Christopher G. Piecuch
Visualization: Kelly McKeon
Writing – original draft: Kelly McKeon
Writing – review & editing: Christopher G. Piecuch

Abstract Compound floods are often thought of as large, infrequent floods during which extremes of coastal sea level and/or river flow combine with each other or additional factors (e.g., tides and rainfall) to induce major flooding. However, little is known about the potentially compound nature of more frequent, lower-level floods. Here, we introduce the term "compound minor floods" to define minor floods composed of two or more water-level sources. We use the Delaware River Estuary as a case study to investigate the prevalence and composition of these minor compound floods along the extent of a tidal river. We apply multiple linear regression to a 22-year time series of coastal water levels and river discharge to establish the contributions of tides, nontidal open-ocean effects, and river discharge to minor flood events at eight locations along the tidal Delaware River. We find that most minor flood events are compound in nature, requiring at least two components (e.g., tides and river discharge) to initiate flooding. We identify spatial structure in the relative importance of oceanographic and riverine contributions to minor flooding along the tidal reach of the estuary. These results suggest that incorporating fluvial components into minor flooding assessments is important to fully characterize flood risk along tidal rivers and estuaries.

Plain Language Summary Compound floods are usually thought of as major floods during which extreme storm surge and extreme river flows happen simultaneously. Less is known about how tides, surges, mean sea level, and river flow might combine to cause minor flooding in the absence of an extreme event. Here, we use 22 years of tide gauge observations from eight locations along the tidal portion of the Delaware River to understand how coastal water level and river discharge may contribute to minor compound floods under nonextreme conditions. We find that most minor floods in the Delaware River Estuary are compound floods. We show that river discharge contributes to minor flooding at all locations along the river, but its influence on floods is most important in the upper estuary. Our results motivate river discharge being considered as a flood component in assessments of future minor flood risk in tidal rivers and estuaries.

1. Introduction

Tidal rivers and estuaries are unique locations that experience flooding from both oceanographic and riverine origins. At the intersection of fluvial and coastal flooding are compound floods, which are caused by two or more flood drivers, such as storm surge and rainfall (Ganguli & Merz, 2019; Moftakhari, Salvadori, et al., 2017; Muñoz et al., 2022; Wahl et al., 2015). Past studies have explored the mechanisms behind major compound floods with return periods of decades to centuries, while less is known about the nature of lower-level but potentially more frequent compound minor floods (Bevacqua et al., 2020; Ghanbari et al., 2021; Moftakhari, Salvadori, et al., 2017; Serafin et al., 2019; Wahl et al., 2015; Ward et al., 2018). Often, so much human life and resources are concentrated along shorelines that the cumulative socioeconomic impact of minor floods may exceed losses from infrequent extreme events (Campbell et al., 2021; Fant et al., 2021; Hino et al., 2019; Moftakhari, AghaKouchak et al., 2017; Moftakhari et al., 2018). Consequently, characterizing the nature of minor compound flooding along the full extent of the estuary is needed to understand flood risk in tidal rivers.

Days of high-tide flooding have been increasing along the Mid-Atlantic coast since 1950, with pronounced acceleration over the past 20 years (Li et al., 2022; Sweet et al., 2021). Li et al. (2022) decomposed water-level time series from 120 tide gauges around the United States into five components of (a) sea-level rise, (b) seasonal variability, (c) tidal anomaly, (d) interannual to decadal variability, and (e) nontidal residuals, to better understand the causes of high-tide floods around the country. They found that nontidal residuals were required for 60% of high-tide floods to occur along the Mid-Atlantic Coast. However, Li et al. (2022) did not probe the composition of

the nontidal residual component, which encompasses a variety of high-frequency processes including (but not limited to) wind-driven storm surge, wave setup effects, the inverted barometer effect, as well as the impacts of precipitation and river discharge. Better understanding of minor flooding in estuarine regions requires a more granular accounting of the relative roles of these processes, particularly river discharge.

Past work has developed and tested hydrodynamic models under conditions of compound extremes in tidal rivers, including the Delaware (Bakhtyar et al., 2020; Kerns & Chen, 2023; Ye et al., 2020). Such work often seeks to reproduce known flood events in models to create and improve probabilistic flood hazard assessments (Orton et al., 2020). Others have used statistical dependence structures (Ghanbari et al., 2021; Wahl et al., 2015; Ward et al., 2018) and idealized analytical models (Familkhalili et al., 2022) to understand the relative importance of riverine versus ocean effects on extreme flooding in estuaries and tidal rivers. However, few studies have used observational approaches to interrogate relationships between upstream and downstream tidal river components of nonextreme water levels, including high-tide floods (Baranes et al., 2023). The availability of water-level observations with high spatiotemporal resolution makes the Delaware River Estuary an ideal location to explore incidences of nonextreme compound floods.

Previous work on compound floods suggested that there is an along-river transition zone where water levels upstream of the transition zone are dominated by river discharge and water levels downstream of the transition zone are dominated by sea level, with the specific location dependent on estuary geometry and river volume (Bermúdez et al., 2021; Bilskie & Hagen, 2018; Kerns & Chen, 2023; Serafin et al., 2019). However, it is unknown to what extent this relative upstream/downstream dominance of discharge/sea level applies during conditions of nonextremes.

Here, our goal is to use observations to better understand the potential compound effects of oceanographic and riverine processes on minor floods in a tidal river. We investigate three components of minor floods in the Delaware River: astronomical tides, nontidal open-ocean effects, and river discharge. We pay particular attention to the spatial gradient of floods related to these simultaneous coastal and riverine processes. Several terms exist for low-magnitude floods including minor floods, high-tide floods, nuisance floods, and sunny day floods (Moftakhari et al., 2018). Recent literature (e.g., Sweet et al., 2021; Thompson et al., 2021) has used the term "high-tide flood" to define minor flooding, occasionally with the clarification that this term does not mean all high-tide floods happen at high tide, or that tides alone responsible for flooding (e.g., Hague & Taylor, 2021; Li et al., 2022; Piecuch et al., 2022). The term high-tide flood is used ubiquitously to describe low-level flooding because current methods for defining, monitoring, and setting flood thresholds are based on tide gauge data (Sweet et al., 2021). Here, we also utilize river-gauge data to characterize incidents of low-level flooding and as such choose to use the "minor flood" terminology over the "high-tide flood" terminology. Moving forward, the term "compound minor flood" signifies a flood event in which none of the examined flood drivers were in an extreme state (as defined immediately below), but nevertheless, a flood was observed (Figure 1).

In statistics, the term "extreme" is often used to describe events that fall in the tail end of a distribution that are unusual, scarce, or rare, and that may or may not have human impacts (e.g., annual maximum water level, 100-year water level, etc.) (Coles, 2001). Here, we instead use the term "extreme" or "compound extreme" to indicate a flood event in which one or more flood components were independently above a threshold based on impacts. Such events tend to be associated with the highest water levels observed over the study period (above the 99th percentile of the still water-level distribution) (Figure S1 in Supporting Information S1). In contrast, a "compound minor flood" is a flood where still water level exceeds the threshold, but none of the contributing processes are extreme in the sense just described. We illustrate the difference between what we declare a "compound extreme" and a "compound minor flood" in Figure 1, which depicts the time series of water-level components during two floods affecting the lower (Ship John Shoal), middle (Marcus Hook), and upper (Burlington) estuary.

This work addresses three primary research questions: (a) What percentage of floods observed in the Delaware River Estuary over the past two decades are compound minor floods? (b) What are the relative contributions of tides, river discharge, and coastal sea level to minor flooding along the Delaware River? (c) How do the answers to questions (a) and (b) vary at tide gauges along the extent of the estuary?

To answer these questions, we use publicly available data sets from tide and streamflow gauges to describe the relationship between coastal sea level, river discharge, and minor floods along the Delaware River Estuary (Section 2.2). We apply multiple linear regression to the observational time series of water levels at the coast and

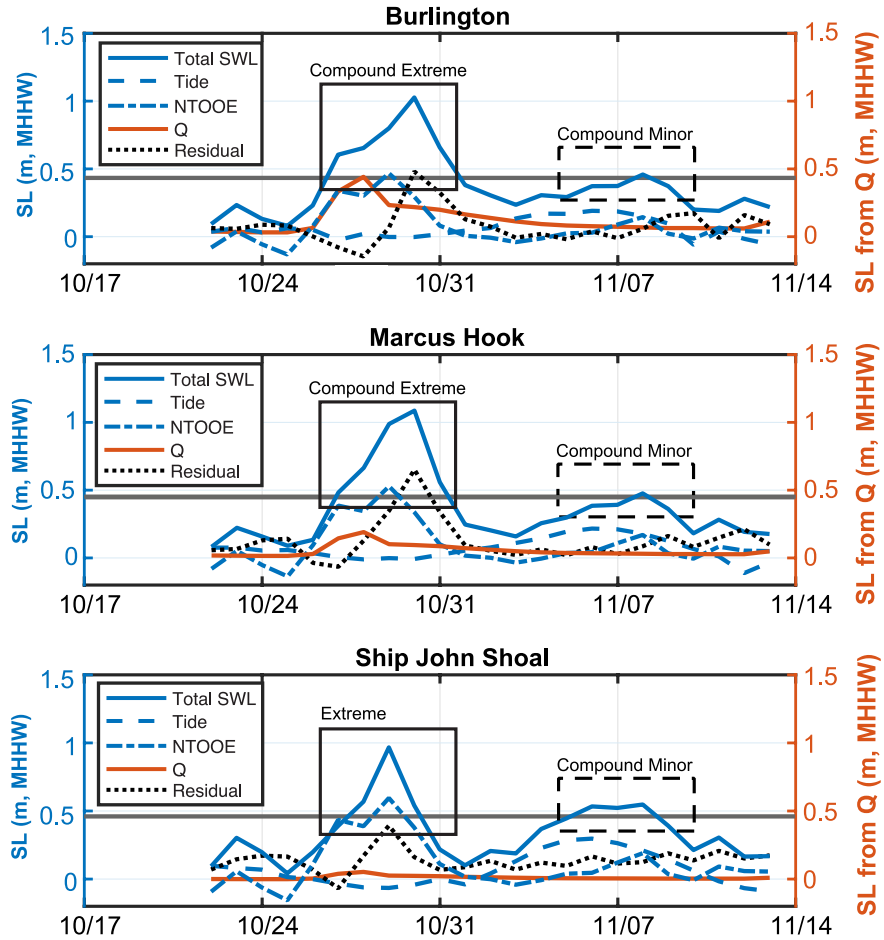

Figure 1. Water levels from two representative flooding events in 2021 at Ship John Shoal (downstream), Marcus Hook (mid-river), and Burlington (upstream), separated into the flood components considered in this analysis (Figure 2, Equation 1). Observed daily maximum still water level (total SWL) is represented by the solid blue line. Water-level contributions from astronomical tides are indicated by the dashed blue line. Water-level contributions from nontidal open-ocean effects (NTOOE) and the regression residual are determined by Equation 1 and represented by the dotted blue line and dotted black line, respectively. Water-level contributions from river discharge (Q) are determined by Equation 1 and plotted in red on the right y-axis. All components (tide, NTOOE, Q, and residual) are plotted independent of mean sea level, which is included only in the total SWL line. The flood threshold (m, MHHW) at each site is plotted in gray. The first peak in water level at Burlington (29 October 2021, black box) represents what we refer to as a "compound extreme," in which water-level contributions from NTOOE, Q, and residual, are greater than the flood threshold, and thus independently sufficient to initiate flooding. The dashed black box (8 November 2021) illustrates what we refer to as a compound minor flood, where none of the water-level drivers (tide, NTOOE, Q, and residual) cross the flood threshold on their own (referred to as "nonextreme" in the text), but the sum of their water-level contributions causes a minor flood.

discharge upriver (Section 2.3). We isolate days of flooding at eight locations along the tidal reach of the river and decompose water levels during floods into oceanic and riverine components (Section 2.4). We find that most floods in the Delaware Estuary are indeed compound minor floods, with the number and composition dependent on position within the estuary.

2. Data and Methods

2.1. Study Site

The Delaware River Estuary on the Mid-Atlantic coast is home to over eight million people (Partnership for the Delaware Estuary, 2022b) and a $12 billion industrial region (Partnership for the Delaware Estuary, 2022a). At 530 km in length, the Delaware River is the longest undammed river on the United States East Coast, with an average annual discharge of 330 $m^3 s^{-1}$ (Bakhtyar et al., 2020; Pareja-Roman et al., 2020). Roughly 58% of mean

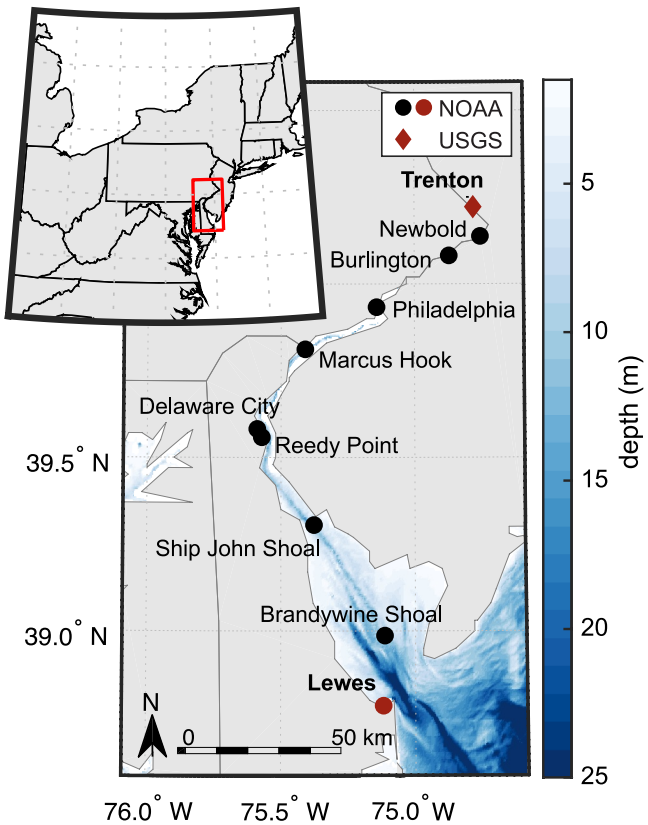

Figure 2. Study region. Black symbols mark upstream tide gauges. Red symbols mark gauges used as boundary conditions. Circles signify National Oceanic and Atmospheric Administration tide gauges, and the diamond signifies the United States Geological Survey streamflow gage. The red box in the inset map delineates the study area. River depth is shown in blue (GEBCO, 2022).

annual freshwater flux (~570 m^3 s^{-1}) to the Delaware Bay is from the Delaware River north of Trenton. The Schuylkill (~77 m^3 s^{-1}) and Christina (~19 m^3 s^{-1}) rivers account for an additional ~17%, while the remaining fluxes are from other sources, each contributing less than 1% individually (Bakhtyar et al., 2020; Pareja-Roman et al., 2020; Sharp, 1984; Whitney & Garvine, 2006). The estuary is 240 km long, extending from the head of tides at Trenton, NJ, to the bay mouth between Lewes, DE, and Cape May, NJ (Figure 2). The tidal regime is semidiurnal, dominated by the M_2 constituent, with a mean tidal range between 1.2 m at Lewes, DE, and 2.6 m at Newbold, PA. The estuary widens exponentially from the head to the mouth, with a width of ~0.3 km at Trenton and ~45 km at Lewes and a mean depth of ~5–10 m (Pareja-Roman et al., 2020). Sea-level rise along the extent of the river is ~3–4 mm per year over the past century (Sweet et al., 2022).

2.2. Data

The tidal extent of the Delaware River is well gauged, making it a suitable location to characterize the spatial structure of compound minor floods along an estuary. We use hourly still water-level observations and station datums from nine National Oceanic and Atmospheric Administration (NOAA) tide gauges between Lewes, DE, and Newbold, NJ, and daily mean discharge data from the United States Geological Survey (USGS) streamflow gage at Trenton (Figure 2, Table 1). We consider data from 2002 to 2023, during which all gauges have complete or near-complete hourly water-level time series. Harmonic analysis was performed on the hourly still water-level time series to obtain tidal predictions. The daily maximum water level and the daily maximum predicted tide were both taken from their respective hourly time series.

2.2.1. Tidal Predictions

The predicted tide at each gauge was derived from a year-by-year harmonic analysis with the UTide MATLAB package applied to hourly observed water levels at each gauge (Codiga, 2011). The linear trend in hourly water-level observations was removed prior to harmonic analysis. The analysis was

Table 1
Gauges Included in This Study

Location	Gauge id	MHHW (above MSL)	Flood threshold (above MHHW)	Number of floods
Lewes	NOAA 8557380	0.7380	N/A	N/A
Brandywine Shoal	NOAA 8555889	0.8790	0.5166	163 ± 26
Ship John Shoal	NOAA 8537121	0.9650	0.4650	434 ± 41
Reedy Point	NOAA 8551910	0.8900	0.4150	266 ± 32
Delaware City	NOAA 8551762	0.9280	0.4560	244 ± 32
Marcus Hook	NOAA 8540433	0.9230	0.4530	247 ± 32
Philadelphia	NOAA 8545240	0.9760	0.4610	291 ± 35
Burlington	NOAA 8539094	1.1760	0.4490	364 ± 37
Newbold	NOAA 8548989	1.2390	0.5690	134 ± 23
Trenton	USGS 01463500	N/A	N/A	N/A

Note. Mean high high water (MHHW) is listed as meters above mean sea level (MSL) at each gauge. Flood thresholds reported are NWS minor flood thresholds (m above MHHW), except for Brandywine Shoal and Ship John Shoal, which are mean values determined in Mahmoudi et al. (2024). The number of floods indicates the number of days the maximum daily water level was above the threshold, reported as the bootstrapped mean ± 2σ (see Sections 2.4, 2.5).

first run on "auto" with all constituents included on 3-year windows of detrended sea-level observations where only the middle year was reconstructed (Codiga, 2011). If more than 25% of hourly water-level observations were missing from this period, it was expanded to 5 years except at Brandywine Shoal, where the entire time series was used. To accurately represent the seasonal cycle represented by the combination of long-period solar annual (Sa), solar semiannual (Ssa) tidal constituents, and mean sea level (MSL), the year-by-year tidal reconstruction was subtracted from the full 22-year water-level time series and a second harmonic analysis of only annual and semiannual components was performed on the 22-year nontidal residual time series. The tidal reconstructions from both harmonic analyses were then summed to obtain the tidal prediction. The linear trend that was removed from the water level prior to harmonic analysis was added back to the tidal predictions such that sea-level rise is included in the predicted tide for the purpose of this analysis. Including the linear trend in the tidal prediction would serve to emphasize the role of tides in minor flooding over time, although changes through time are not addressed in this study. In the flood classification method used here, this choice serves to highlight tide-only floods in the sense of Hague and Taylor (2021), who use tide-only inundation as a metric to describe the role of sea-level rise in minor floods resulting from high still water levels.

UTide predictions were selected over predictions provided by NOAA because currently available tidal predictions are based on data over 1983–2001, whereas observations used here begin in 2002. Further, the river section between Lewes and Philadelphia was dredged in sections between 2010 and 2022 to increase the channel depth by 1.5 m. Sections between Trenton and Philadelphia have also been dredged intermittently between 2022 and 2024 (USACE, 2022). An annual tidal analysis captures dredging related changes in tidal amplitude within the tidal component.

2.2.2. Flood Thresholds

The National Weather Service (NWS) minor flood thresholds are used to define floods throughout this record because of their association with observable flood water impacts (e.g., the number and extent of roads flooded in proximity to the gauge). However, NWS does not provide thresholds for Brandywine Shoal Light or Ship John Shoal because these gauges are located on lighthouses in the widest part of the estuary, where it is difficult to quantify flood impacts. For these sites, we use mean high-tide flood thresholds from Mahmoudi et al. (2024), which were determined using a machine learning algorithm designed to produce spatially continuous, impact-based flood thresholds (Table 1). Note that flooding described here is related to still water levels recorded at tide gauges, and any flooding due to wave-related processes falls outside the scope of this study.

2.3. Regression

We employ multiple linear regression to relate daily maximum water level at eight upstream tide gauges to daily maximum water level at the open coast (Lewes, DE) and daily mean discharge at the head of tides (Trenton, NJ) over 2002–2023 (Figure 2). Any day in the 22-year time series with one or more variables' missing data was excluded from the analysis. The means of all variables were removed prior to regressing, effectively removing MSL from the regression. MSL ($\overline{\zeta}$) is defined for each site individually as the 22-year time series mean and was added back in the flood classification step (see below). Our model is

$$\zeta(x,t) - T(x,t) = a(x)\zeta_0(t) + b(x)\,Q(t) + \epsilon(x,t) \tag{1}$$

where ζ is the daily maximum water level, T is the daily maximum predicted tide, x is the upstream gauge location, t is the time, a and b are location-dependent constants, ζ_0 is the daily maximum nontidal water level at Lewes, Q is daily mean discharge at Trenton, and ϵ is the residual, which includes errors and unmodeled processes; see Section 3.2 for further discussion of the residuals and their interpretation. Nontidal water level ζ_0 was determined by subtracting the predicted tide from the observed water level at Lewes. We use "nontidal open-ocean effects" in reference to the term $a\zeta_0$ to signify that the predicted astronomical tide has been removed from the water-level signal at the most seaward gauge (Lewes), but we do not distinguish between other sea-level processes operating on variable frequencies.

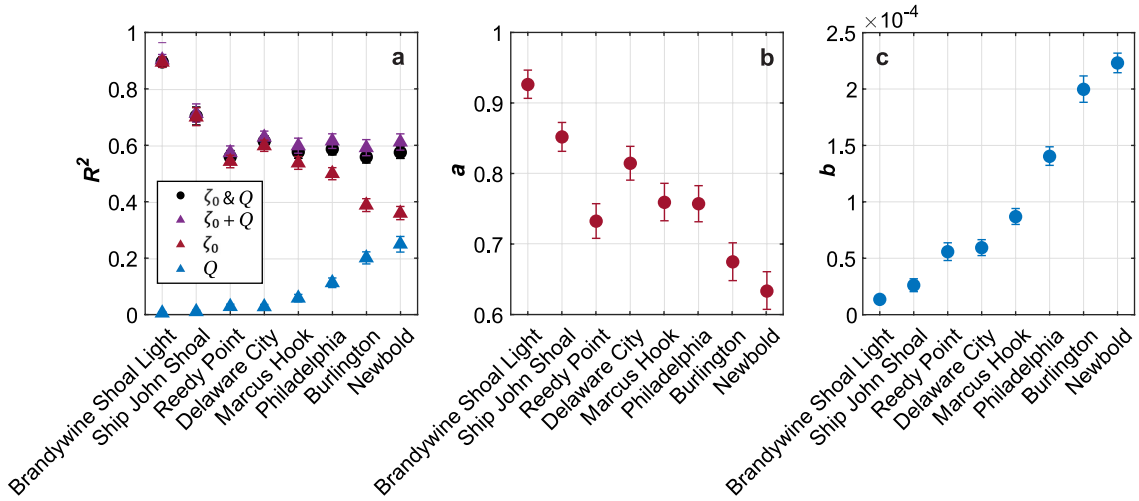

Figure 3. Solutions to Equation 1. In all plots, the most downstream site is on the left of the *x*-axis, and the most upstream site is on the right of the *x*-axis. Error bars denote 95% confidence intervals from bootstrapping. (a) *R*-squared values from multiple regression are shown in black circles. *R*-squared values of single linear regressions are shown in red (nontidal open-ocean effects at Lewes, ζ_0) and blue (discharge at Trenton, Q) with their sum in purple, (b) regression coefficient a associated with nontidal open-ocean effects at Lewes (ζ_0) from Equation 1, and (c) regression coefficient b (m m^{-3} s) associated with discharge at Trenton (Q) from Equation 1.

2.3.1. Time Lags

The observed tidal lag between Lewes and Trenton is approximately 8 hr. Because we use daily data, we expect the influence of phase lags between variables due to wave propagation to be reduced. To test this, we also performed a regression analysis that included the Hilbert transforms of ζ_0 and Q as additional predictors (Equation S1 in Supporting Information S1). The Hilbert transform induces a phase shift of 90° to every frequency component of the predictor-variable time series. By including ζ_0 and Q and their respective Hilbert transforms in the model, we permit more general phase relationships between variables to be captured. This contrasts with the model in Equation 1, which only allows perfectly in-phase or out-of-phase relationships (Piecuch et al., 2022). We determined that both models performed comparably well in terms of explaining data variance, which is consistent with our expectation that phase lags do not play a leading role on the timescales being considered (Figure S2 in Supporting Information S1). Therefore, we proceeded with Equation 1 and omitted the Hilbert transforms of the predictor variables. We also performed a lagged correlation analysis between variables. When performing this analysis over a series of daily time lags (0–4 days), we found that R^2 values decreased substantially for longer time lags from 1 to 4 days. As such, time lags between upstream and downstream processes do not appreciably impact these results.

2.3.2. Independence of Boundary Conditions

The Delaware River's lack of upstream damming, simple estuarine geometry, and shallow-convergent morphology all allow a simple linear method to be appropriate for this analysis as the boundary conditions ζ_0 and Q are sufficiently weakly correlated with one another ($R^2 = 0.005$ and $p < 0.001$) to represent independent predictors (Pareja-Roman, 2020; Van Rijn, 2011). This was corroborated by performing ordinary linear regressions between individual independent variables (ζ_0 and Q) with the dependent variable ($\zeta - T$) at each site separately and summing their coefficients of determination (R^2 values). The variance explained by the summed individual linear regressions is comparable to the R^2 values determined by multiple linear regression, which suggests a lack of multicollinearity between variables (See Section 3.1, Figure 3a). To validate the assumption of homoscedasticity (equal variances between predictors), we performed a Breusch-Pagan test by regressing the squared model residuals with each independent predictor within the bootstrapping framework and found no correlations larger than 0.02 ± 0.009 (Breusch & Pagan, 1979). These results suggest that very little of the residual variance could be explained by river discharge and nontidal open-ocean effects.

We also calculated the rank correlation coefficient Kendall's τ between the two boundary conditions (as in Wahl et al., 2015), which was found to be 0.0614, and $p < 0.0001$. Other correlation metrics including Spearman's

correlation coefficient returned similar values. With a statistically significant value > 0, we cannot reject the null hypothesis that the predictors are entirely uncorrelated ($\tau = 0$), although a correlation less than 0.1 indicates a weak to negligible correlation between variables (Schober et al., 2018). However, the influences of the boundary conditions (ζ_0 and Q) on the dependent variable at each site ($\zeta - T$) may not be independent. Specifically, even though we assume linear relationships in this regression model, nonlinear dependencies between the predictor variables are also likely to influence along-river water level. Nevertheless, the model presented here explains a majority of nontidal daily maximum sea-level variance and is thus a useful approach to describing the relationship between upstream river discharge and downstream sea level in the Delaware River Estuary.

2.4. Flood Classification

We take a peaks-over-threshold approach to identifying flood days. Following past studies (e.g., Sweet et al., 2022; Thompson et al., 2021), we consider a flood as any day in the observational time series that the daily maximum still water level exceeds the flood threshold. After isolating the flood days, the contributions of each of the four water-level components (T, $a\zeta_0$, bQ, and ϵ) were determined for those days of flooding. We then categorized floods based on the minimum number of water-level components that could be combined to exceed the flood threshold. The MSL ($\overline{\zeta}$) that was removed during the regression process was added back to each sum of components and treated as the baseline level. Note that the linear sea-level rise trend and seasonal cycle are included in the tidal component of this analysis.

Floods when one component was enough to initiate flooding (e.g., tides alone exceeded the flood threshold) were classified as single-component floods and removed from further classification. Remaining floods wherein the sum of two or more components were required to meet the flood threshold, but none of those components could have caused flooding independently, are considered compound minor floods. Compound minor floods were separated into categories of two, three, and four components, where if two components could be summed to exceed the threshold, the flood was excluded from further classification as a three- or four-component flood. This method ensures that each flood is counted only once in each flood category such that the total number of floods of the four categories (one-, two-, three-, and four-component) sums to the overall number of floods.

After categorizing each flood event by the number of components, we consider which elements of $a\zeta_0$, bQ, and ϵ (or combinations thereof) may be responsible for each event. For each event at each site, we assign a binary value to each possible combination of elements: a value of one is assigned if the specific combination of variables can be summed to exceed the threshold, a value of zero is assigned otherwise. The result is a site-specific binary matrix of size $m \times n$, where m is the number of flood events at that site and n is the number of variable combinations ($n = 15$, see Figure 5b for possible combinations). Each row is then divided by the total number of possible flood combinations for that event. The resulting matrix is then consolidated into a single row for each site. This is accomplished by summing the values over each column and normalizing by the total number of flood events at the site to produce a percentage value for each element combination (Figure 5b).

2.5. Uncertainty Quantification

We use bootstrapping to quantify uncertainties in flood classification related to the limited number of flood days in the observational record. To perform bootstrapping, we first randomly select (with replacement) a set of indices with the same length as the observational time series. We then generate a set of new time series for river discharge, water level, and predicted tide, by taking the contemporaneous data values from each observational time series at the randomly generated index points. We then go through the process of multiple linear regression and event classification according to Sections 2.3 and 2.4 with each of the randomly generated time series. We repeat this entire process 1000 times, such that we create 1000 sets of results. Values reported represent means and 95% confidence intervals of these 1000 iterations. This method quantifies only sampling uncertainty, and the actual range of uncertainty is likely to be larger than the confidence intervals reported here (Abbaszadeh et al., 2022).

To test for the influence of autocorrelation on the results, we also performed this analysis using phase scrambling (as in Li et al., 2022) as well as block bootstrapping, and we found results were largely the same across all three methods. Thus, for simplicity, we use ordinary bootstrapping for the results shown here.

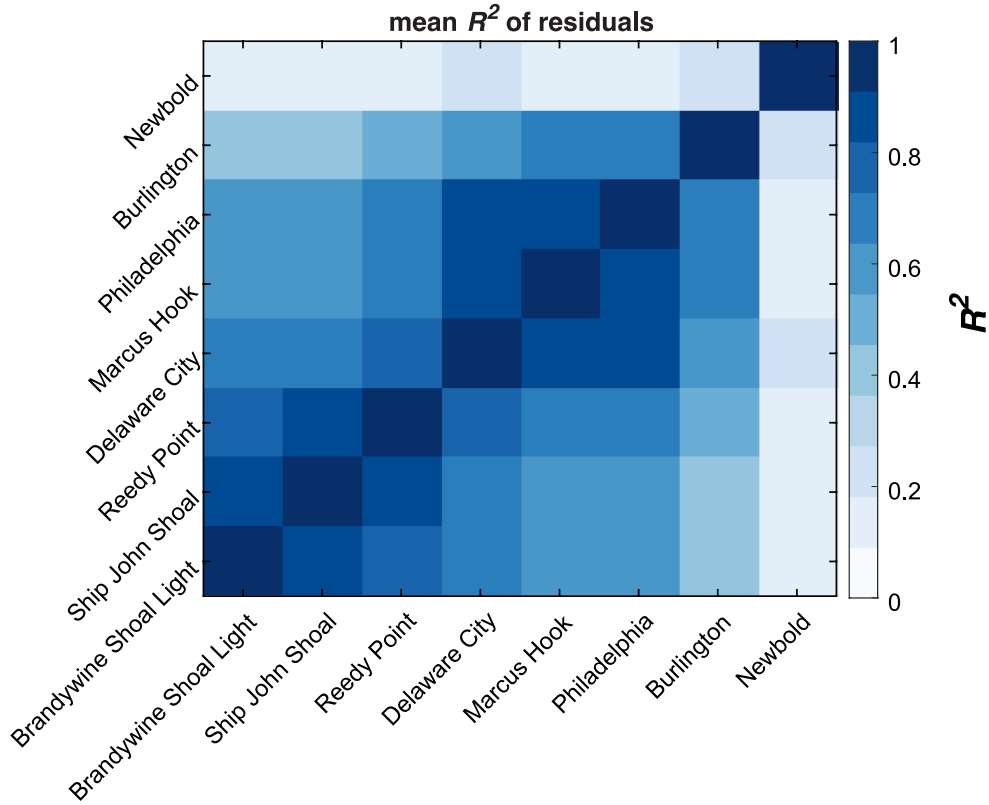

Figure 4. Mean of bootstrapped R^2 values from cross-correlations computed between pairs of residual time series as a function of the site pairs. Distance from Lewes increases from the bottom to the top on the *y*-axis and left to right on the *x*-axis.

3. Results

3.1. Linear Regression

The ordinary least squares solution to Equation 1 yields two sets of regression coefficients with distinct spatial structures (Figure 3). Regression coefficients a associated with nontidal open-ocean effects range from 0.93 ± 0.02 downstream to 0.63 ± 0.03 upstream. Regression coefficients b associated with discharge range from $1.35 \times 10^{-5} \pm 3.1 \times 10^{-6}$ m m^{-3} s to $2.23 \times 10^{-4} \pm 8.56 \times 10^{-6}$ m m^{-3} s upstream. A downstream a coefficient $\sim$1 demonstrates that downstream locations experience the full impact of nontidal open-ocean effects while upstream values $<<$ 1 suggest that nonlinear effects and frictional processes damp the communication of the open-ocean signal upstream. Likewise, lower b coefficients downstream are consistent with the intuition that water level becomes less sensitive to a given river flow variation with distance downstream.

Coefficients of determination (R^2) for the multiple regression model range from 0.90 ± 0.02 at the most downstream site to 0.58 ± 0.02 at the most upstream site. This is consistent with the sum of the R^2 values from simple linear regressions of each of the predictor variables independently. R-squared values associated with ζ_0 alone range from 0.36 ± 0.023 upstream to 0.90 ± 0.19 downstream. Conversely, R^2 values associated with Q alone range from 0.008 ± 0.005 at Brandywine Shoal Light to 0.252 ± 0.028 at Newbold (Figure 3a). Other statistics designed to incorporate bias were also assessed. However, because time-mean values were removed from all time series prior to regressing, the effect of bias in the R^2 statistic is already reduced. This is evident in the results of the Nash-Sutcliffe efficiency test, which were identical to the R^2 values. The Kling-Gupta efficiency (KGE) test also yielded positive values at all sites, ranging from 0.51 ± 0.03 to 0.89 ± 0.02 (Gupta et al., 2009). Note that, because all time series have zero mean, KGE values computed here measure correlation and variability bias. These results suggest that 58%–90% of the daily nontidal along-river water variability can be explained with just two predictor variables of river discharge and nontidal open-ocean effects.

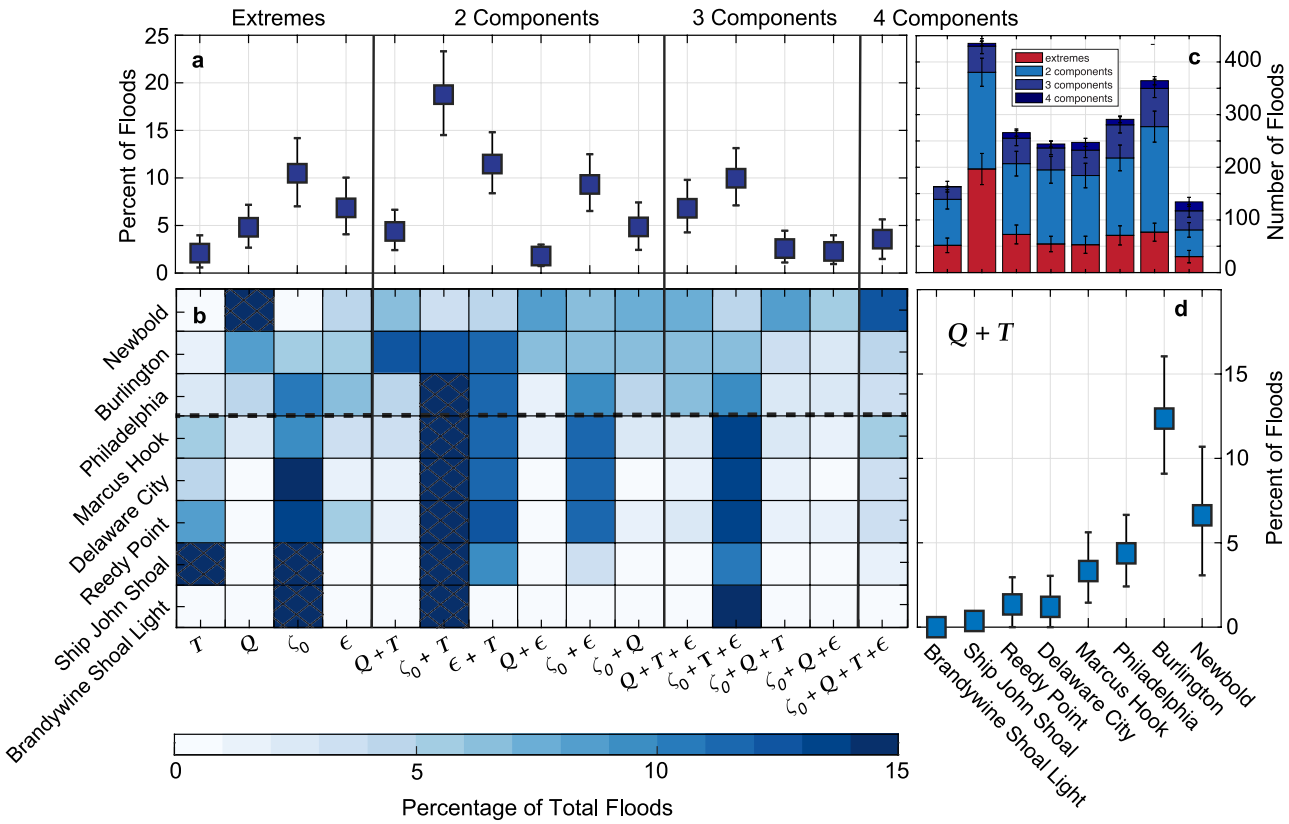

Figure 5. All possible combinations of flood components are shown on the *x*-axis of panels a and b. Solid black lines mark the separation between single-component floods (left), two-component floods, three-component floods, and four-component floods (right). (a) Mean percentage of total floods occurring at Philadelphia that can be explained by the components on the *x*-axis. Error bars represent 95% confidence intervals determined by bootstrapping. (b) Sites on the *y*-axis increase in distance from the coast from the bottom to the top. Shading represents the mean percentage of total floods occurring at each site that can be explained using the components on the *x*-axis. Cross-hatching denotes percentages over 15%. The dashed black line marks the distinction between upstream and downstream sites. *X*-axis for panels c and d show sites ordered from the most downstream on the left to the most upstream on the right. (c) Mean number of floods in each component class at each site. Single component floods are shown in red. Shades of blue indicate compound minor floods. Error bars are 95% confidence intervals from bootstrapping. (d) Mean percentage of floods at each site that could be explained by discharge (Q) and tides (T). Error bars denote 95% confidence intervals from bootstrapping.

3.2. Residuals

Variability in along-river water level not captured by astronomical tides, nontidal open-ocean effects, or river discharge, appears in the residual term (ϵ) of Equation 1. Cross-correlations computed between pairs of residual time series show decreasing R^2 values with increasing distance between sites (Figure 4). This local-to-regional spatial structure could possibly be related to along-river winds, surface runoff, or direct precipitation, which are not included in the regression. For example, the average residual time series across tide gauges is correlated with sea-level pressure over the western subtropical North Atlantic Ocean and anticorrelated with pressure over the Great Lakes region (Figure S4 in Supporting Information S1). The signs of these correlations suggest along-river winds may play a role, but their magnitudes are modest, representing only part of the residual story. The residuals may also reflect tidal changes, nonlinear interaction between the ocean and upstream boundary conditions, or nonlinear amplification of the boundary conditions absent from our model. Because of this, we consider the residuals as an independent component of compound minor floods, but do not attempt to definitively attribute this component to any particular process.

3.3. Spatial Structure of Compound Minor Floods

The total number of flood days between 2002 and 2023 ranged between ~135 days (Newbold) and ~435 days (Ship John Shoal). The average daily maximum water level during days of flooding at all sites except Newbold

was between 0.5 and 0.58 m above MHHW. Most floods occurred during spring and fall, consistent with characteristics of high-tide flooding described in the Mid-Atlantic (e.g., Li et al., 2022, 2023).

We find that 55%–79% (95% CI) of total flood days recorded across all gauges required two or more components to exceed the flood threshold and are therefore compound minor floods. At all gauges, the predominant flood observed is the two-component flood, followed by single-component floods, and then three-component floods. The absolute number of four-component floods remains low and spatially consistent throughout the estuary (Figure 5c).

The highest prevalences of compound minor floods are observed at midstream urban centers of Delaware City (72%–83% of floods), Marcus Hook (73%–84% of floods), and Philadelphia (71%–81% of floods) (Figure 5). Extreme events requiring only one component to exceed the flood threshold made up 21%–45% of total observed flood events on average. Of these single-component floods, the majority in the lower river were caused by nontidal open-ocean effects while the majority in the upper river were caused by river discharge (Figure 5b).

The composition of compound minor floods differs with position along the river. As there is a transition in the makeup of compound minor floods inland of Marcus Hook, we refer to sites including and seaward of Marcus Hook as "downstream" sites, while Philadelphia, Burlington, and Newbold will be referred to as the "upstream" sites (Figures 2 and 5b). River discharge contributed to 31 ± 5%, 51 ± 5%, and 75 ± 7% of floods at the upstream sites (Philadelphia, Burlington, Newbold, respectively), while nontidal open-ocean effects contributed to 62 ± 5%, 48 ± 5%, and 51 ± 8% of floods, respectively. River discharge contributions at downstream sites ranged from 1 ± 1% at Brandywine Shoal to 21% ± 5% at Marcus Hook, while downstream nontidal open-ocean effects contributions ranged between 99 ± 2% of floods at Brandywine Shoal and 70 ± 6% of floods at Marcus Hook. Tidal contributions were all between 66 ± 6% and 78 ± 4% at downstream sites, and 49 ± 8% to 60 ± 6% at upstream sites. While the residual portion of floods only contributed to 16% ± 6% and 27% ± 4% at Brandywine Shoal and Ship John Shoal, respectively, the residual term contributed to around 45% of floods at all other sites (Figure 5, Figure S3 in Supporting Information S1).

4. Discussion

4.1. Role of River Discharge in Minor Flooding

The short-term impact of river discharge on coastal flooding under conditions of compound extremes has been studied in detail (e.g., Bakhtyar et al., 2020; Moftakhari, Salvadori, et al., 2017; Serafin et al., 2019; Wahl et al., 2015). Several studies have also interrogated the long-term contributions of river discharge to MSL changes (Durand et al., 2019; Meade & Emery, 1971; Piecuch, 2023; Piecuch et al., 2018; Talke et al., 2020). Each of these studies found that riverine effects can substantially impact water levels at the coast. Our results fill a gap in these findings with respect to the overall magnitude and timescales of river impacts on coastal water levels, demonstrating that river discharge also plays a nontrivial role in the amount of chronic, low-level flooding in the tidal Delaware River and Estuary. Further, our work identifies a spatial gradient in the influence of discharge on estuarine flooding that has been understudied in previous work investigating minor floods at the coast.

Riverine water-level contributions were necessary for some amount of minor flooding at all sites along the extent of the estuary, even at the most downstream sites, where river discharge contributions ranged from 1% ± 1% at Brandywine Shoal to 21% ± 5% at Marcus Hook. In other words, these percentages of floods would not have occurred in the absence of river discharge forcing. Significant work has gone into understanding how the variability of different sea-level components (sea-level rise, nodal cycle, etc.) and morphological changes (dredging, shoreline hardening, etc.) will affect the frequency and magnitude of estuarine flooding (De Leo et al., 2022; Li et al., 2022, 2023; Pareja-Roman et al., 2023; Ralston et al., 2019; Ray & Foster, 2016; Thompson et al., 2021; Woltemade et al., 2020). However, much of this work focuses on oceanic contributions to floods and where discharge is included in flooding assessments, it is often only under conditions of extremes such as hurricanes, extratropical cyclones, and nor'easters. Detailed discussions of riverine contributions to minor floods remain limited among research covering how climate and urbanization relate to high-tide flooding in estuaries (Baranes et al., 2023; De Leo et al., 2022; Pareja-Roman et al., 2023; Talke & Jay, 2020).

An Interagency Task Force Sea Level Rise Technical Report acknowledges the potential contribution of river flow to flooding, as far as its influence is captured in the water levels recorded at tide gauges. However, that report also states that river discharge is not factored into future projections and is thus unaccounted for in NOAA's

annual High Tide Flood Outlook such that future changes in river discharge will not directly lead to changes in high-tide flood predictions (Sweet et al., 2021, 2022). In this report, Philadelphia is predicted to experience 35–65 days of high-tide flooding per year by 2050. This prediction uses a combination of models that incorporate historical flood observations, projections of sea-level rise, harmonic analysis of astronomical tides, and estimates of time-variable climatic phenomenon including the phase of the El Niño-Southern Oscillation and sea surface temperature anomalies. However, it does not include projections of river discharge. By 2050, precipitation in the Delaware River Basin is expected to increase by 5%–10%, and river discharge along with it (Najjar et al., 2009; Williamson et al., 2016; Woltemade et al., 2020). Further, Woltemade et al. (2020) suggest that under future climate scenarios, the peak discharge for floods with short recurrence intervals (<25 years) will increase more than the discharge for extreme floods with longer return periods. Our results indicate that river discharge currently contributes to a third of floods at Philadelphia, which suggests that any future changes in river discharge have the potential to also change the frequency and magnitude of minor floods at this location. This finding underscores the need to consider discharge in future high-tide flood predictions at Philadelphia and elsewhere.

4.2. Implications for Other Tidal Rivers

Here, we find that a majority of minor floods in the Delaware River Estuary are compound flood events. Using this well-gauged estuary as a case study enables the quantification of both the prevalence of compound minor floods and the composition of those floods, especially the riverine component. While other estuaries may lack the density of observations available in the Delaware River, our findings here may apply elsewhere. It is likely that compound minor floods are present in other estuaries, particularly in proximal river systems with similar morphologies such as the Chesapeake Bay, the Hudson River, and the Connecticut River estuaries.

Serafin et al. (2019) defined a transition zone within a tidal river where the dominant control on extreme flood water return level changes from a fluvial to an oceanographic source. In the Pacific Northwest, they found this transition happening within 4 km of the river mouth for the 100-year return level. Bilskie and Hagen (2018) likewise simulated storm surges for hurricane events in the Mississippi River Delta and found this transition zone happening between 5 and 25 km of the shoreline. In the Delaware River, we identified a similar transition zone where fluvial and riverine effects have comparable influence (following Serafin et al., 2019) for minor floods approximately 150 km from the river mouth (Figure 5). The difference in the along-river location of this transition zone may relate to several oceanic and terrestrial factors, including estuary morphology, as Serafin et al. (2019) focused on steep, narrow, estuaries and Bilskie and Hagen (2018) focused on a wide, low-gradient deltaic estuary. Nevertheless, their results are qualitatively consistent with ours; river discharge significantly impacts water levels measured by estuarine tide gauges, with the magnitude of impact dependent on position within the estuary. Work by Baranes et al. (2023) analyzing over 50 gauges in the morphologically complex Sacramento-San Joaquin River Delta also found spatially varying influences of fluvial water-level contributions to daily mean water levels around the estuary. These findings indicate that river effects may also play a role in compound minor floods in other estuaries, even those with disparate river geometries and flow regimes.

4.3. Anthropogenic Estuary Modifications

The Delaware River Estuary has been highly modified since the beginning of the industrial era. The initial channel was dredged between 1850 and 1950, doubling the tidal range in the upper estuary (Pareja-Roman et al., 2020). From 2010 to 2022, the section of river between Lewes and Philadelphia was dredged intermittently to increase the total channel depth by 1.5 m to a depth of 13.7 m, with plans to continue this dredging up to Trenton before the end of 2024 (USACE, 2022; USACE, 2023). Ongoing sea-level rise and shoreline hardening serving to limit the lateral expansion of water has added to this tidal amplification (Lee et al., 2017; USACE, 2022).

Decreasing friction associated with increasing water depth simultaneously amplifies storm surge, while allowing more effective communication of discharge pulses downstream, such that extreme events are muted over a larger stretch of river and risk of severe flooding may eventually be reduced as dredging expands the tidal range (Familkhalili et al., 2020; Pareja-Roman et al., 2020; Ralston et al., 2019). However, in contrast to this dampening water-level response during extreme events, some have suggested amplified tidal ranges have and will lead to an increase in low-level minor flooding (Pareja-Roman et al., 2023; Thompson et al., 2021). Changes in river discharge and storm surge extremes, tidal ranges, and riverbed depth and composition induce and amplify existing nonlinearity in the relationship between the oceanographic and riverine components of water level throughout the

estuary (Cao et al., 2020; Familkhalili & Talke, 2016; Ralston et al., 2019). Here, we have used a linear model to explain the role of these components in minor flooding along the river. While we have not ascribed the residual term to a particular process, it is possible that some of the nonlinear characteristics of these river changes are reflected in the model residuals, which contribute to ~45% of minor floods in the upper estuary. Ultimately, research into how estuary modifications may affect minor floods is limited, and more work will be necessary to understand the effects of river morphology modifications on compound minor floods, including how future dredging plans may impact the results presented here (Li et al., 2021).

5. Conclusions and Future Directions

5.1. Summary

Here, we find that 58%–90% of nontidal water-level variability in the Delaware River Estuary can be explained by a linear combination of nontidal open-ocean effects and river discharge. Results show that most floods in the Delaware River from 2002 to 2023 are indeed compound minor floods. While there are spatial variations in the composition of these floods, oceanographic water-level contributions are the largest and most prevalent component of floods. However, our results also demonstrate daily discharge variability is a critical component of minor floods throughout the estuary. We identify a transition zone approximately 150 km up-estuary where riverine effects on minor floods become more prominent. While most models have studied the interactions of river flow and sea level under extreme conditions, our findings suggest that it is worthwhile to apply hydrodynamic models under nonextreme water-level conditions along the extent of the estuary. Finally, this work highlights the need to consider river discharge in future assessments of high-tide flooding (e.g., Thompson et al., 2021), even at downstream locations and especially in estuarine systems analogous to the Delaware River.

5.2. Future Directions

Occurrences of minor floods have been increasing in the Mid-Atlantic region over the twentieth century (Sweet et al., 2021), and Li et al. (2022) suggest that nontidal residuals are an increasingly important component of these floods. However, the short temporal length of midriver tide gauges used in this study limits our understanding of how along-river compound minor floods have changed over time. Repeating a similar analysis for the Delaware over a longer period with river morphology changes under consideration may yield insights as to how the frequency and composition of compound minor floods have changed with sea-level rise, changing tidal regimes, and anthropogenic modifications to the shoreline, river, and estuary. The Delaware River has a management plan in place that includes dredging the upper estuary, orchestrating the timing of water releases from reservoirs to meet watershed discharge goals, and modifying shorelines and land use to best manage stormwater (DRBC, 2020; USACE, 2022). Understanding how some of these estuary modifications have affected minor floods over the past century may provide valuable perspective on the future occurrences of compound minor floods.

Here, we have shown that compound minor flood events are widespread throughout the Delaware River Estuary. It would also be informative to investigate the pervasiveness of compound minor floods and the importance of river discharge in other estuaries and over longer timescales. This will improve our understanding of how these events have evolved over the past century, how they may be included in future projections of high-tide flooding, and to what extent they occur in other tidal rivers. Lastly, the residual term we describe here may be influenced by a variety of processes (e.g., groundwater discharge, along-river winds, surface runoff, etc.), which may have nonlinear interactions with both riverine and oceanographic components of minor floods and thus warrant further exploration. The use of nonlinear hydrodynamic models along with analysis of ancillary weather and climate data may be useful tools to address the mechanisms controlling the residual term. While these questions fall outside the scope of this study, we believe these are important directions for future work on the topic of compound minor floods.

Data Availability Statement

The data used here were downloaded from the NOAA CO-OPS API (https://api.tidesandcurrents.noaa.gov/api/prod/) and the USGS Water Data for the Nation website (https://waterdata.usgs.gov/nwis/dv?referred_module=sw&site_no=01463500, Site Number 01463500). All NOAA and USGS gauge numbers are found in Table 1. Reanalysis fields (Kalnay et al., 1996) used to produce Figure S4 in Supporting Information S1 were

provided by the WHOI CMIP5 Community Storage Server, Woods Hole Oceanographic Institution, Woods Hole, MA, USA, from their website at http://cmip5.whoi.edu/. Codes used for data downloads and analysis can be found at KM's GitHub website (https://github.com/Kelly-McKeon/CompoundHTF).

Acknowledgments
Support came from the NSF Graduate Research Fellowship Program (awards 2141064 and 1745302; KM), NSF award OCE-2123692 (CGP), and the NASA Sea Level Change Team (awards 80NSSC20K1241 and 80NM0018D0004; KM, CGP). We thank Phil Thompson for comments on an early draft of this manuscript and Thomas Wahl for suggestions related to tidal analysis. We acknowledge Dr. Hamed Moftakhari and two anonymous reviewers for their thoughtful suggestions, which improved the manuscript.

References

Abbaszadeh, P., Muñoz, D. F., Moftakhari, H., Jafarzadegan, K., & Moradkhani, H. (2022). Perspective on uncertainty quantification and reduction in compound flood modeling and forecasting. *iScience*, *105201*(10), 105201. https://doi.org/10.1016/j.isci.2022.105201

Bakhtyar, R., Maitaria, K., Velissariou, P., Trimble, B., Mashriqui, H., Moghimi, S., et al. (2020). A new 1D/2D coupled modeling approach for a riverine-estuarine system under storm events: Application to Delaware River Basin. *Journal of Geophysical Research: Oceans*, *125*(9). https://doi.org/10.1029/2019JC015822

Baranes, H., Dykstra, S. L., Jay, D. A., & Talke, S. A. (2023). Sea level rise and the drivers of daily water levels in the Sacramento-San Joaquin Delta. *Scientific Reports*, *13*(1), 22454. https://doi.org/10.1038/s41598-023-49204-z

Bermúdez, M., Farfán, J. F., Willems, P., & Cea, L. (2021). Assessing the effects of climate change on compound flooding in coastal river areas. *Water Resources Research*, *57*(10). https://doi.org/10.1029/2020WR029321

Bevacqua, E., Vousdoukas, M. I., Zappa, G., Hodges, K., Shepherd, T. G., Maraun, D., et al. (2020). More meteorological events that drive compound coastal flooding are projected under climate change. *Communications Earth and Environment*, *1*, 47. https://doi.org/10.1038/s43247-020-00044-z

Bilskie, M. V., & Hagen, S. C. (2018). Defining flood zone transitions in low-gradient coastal regions. *Geophysical Research Letters*, *45*(6), 2761–2770. https://doi.org/10.1002/2018GL077524

Breusch, T. S., & Pagan, A. R. (1979). A simple test for heteroscedasticity and random coefficient variation. *Econometrica*, *47*(5), 1287–1294. https://doi.org/10.2307/1911963

Campbell, L. K., Cheng, H., Svendsen, E., Kochnower, D., Bunting-Howarth, K., & Wapnitsky, P. (2021). Living with water: Documenting lived experience and social-emotional impacts of chronic flooding for local adaptation planning. *Cities and the Environment*, *14*(1). https://doi.org/10.15365/cate.2021.140104

Cao, Y., Zhang, W., Zhu, Y., Ji, X., Xu, Y., Wu, Y., & Hoitink, A. J. F. (2020). Impact of trends in river discharge and ocean tides on water level dynamics in the Pearl River Delta. *Coastal Engineering*, *157*, 103634. https://doi.org/10.1016/j.coastaleng.2020.103634

Codiga, D. L. (2011). *Unified tidal analysis and prediction using the UTide matlab functions*. Technical Report 2011-01. Graduate School of Oceanography, University of Rhode Island. Narragansett RI. 59pp Retrieved from https://www.po.gso.uri.edu/pub/downloads/codiga/pubs/2011Codiga-UTide-Report.pdf

Coles, S. (2001). *An introduction to statistical modeling of extreme values*. Springer.

Delaware River Basin Commission (DRBC). (2020). Delaware River Basin compact. *Delaware River Basin Commission*. Retrieved from https://www.nj.gov/drbc/library/documents/compact.pdf

De Leo, F., Talke, S. A., Orton, P. M., & Wahl, T. (2022). The effect of harbor developments on future high-tide flooding in Miami, Florida. *Journal of Geophysical Research: Oceans*, *127*(7). https://doi.org/10.1029/2022JC018496

Durand, F., Piecuch, C. G., Becker, M., Papa, F., Raju, S. V., Khan, J. U., & Ponte, R. M. (2019). Impact of continental freshwater runoff on coastal Sea Level. *Surveys in Geophysics*, *40*(6), 1437–1466. https://doi.org/10.1007/s10712-019-09536-w

Familkhalili, R., & Talke, S. A. (2016). The effect of channel deepening on tides and storm surge: A case study of Wilmington, NC. *Geophysical Research Letters*, *43*(17), 9138–9147. https://doi.org/10.1002/2016GL069494

Familkhalili, R., Talke, S. A., & Jay, D. A. (2020). Tide-storm surge interactions in highly altered estuaries: How channel deepening increases surge vulnerability. *Journal of Geophysical Research: Oceans*, *125*(4). https://doi.org/10.1029/2019JC015286

Familkhalili, R., Talke, S. A., & Jay, D. A. (2022). Compound flooding in convergent estuaries: Insights from an analytical model. *Ocean Science*, *18*(4), 1203–1220. https://doi.org/10.5194/os-18-1203-2022

Fant, C., Jacobs, J. M., Chinowsky, P., Sweet, W., Weiss, N., Sias, J. E., et al. (2021). Mere nuisance or growing threat? The physical and economic impact of high tide flooding on US road networks. *Journal of Infrastructure Systems*, *27*(4), 04021044. https://doi.org/10.1061/(ASCE)IS.1943-555X.0000652

Ganguli, P., & Merz, B. (2019). Trends in compound flooding in northwestern Europe during 1901–2014. *Geophysical Research Letters*, *46*(19), 10810–10820. https://doi.org/10.1029/2019GL084220

GEBCO Compilation Group. (2022). GEBCO 2022 grid. https://doi.org/10.5285/e0f0bb80-ab44-2739-e053-6c86abc0289c

Ghanbari, M., Arabi, M., Kao, S., Obeysekera, J., & Sweet, W. (2021). Climate change and changes in compound coastal-riverine flooding hazard along the U.S. Coasts. Earth's *future*. *Earth's Future*, *9*(5). https://doi.org/10.1029/2021EF002055

Gupta, H. V., Kling, H., Yilmaz, K. K., & Martinez, G. F. (2009). Decomposition of the mean squared error and NSE performance criteria: Implications for improving hydrological modelling. *Journal of Hydrology*, *377*(1–2), 80–91. https://doi.org/10.1016/j.jhydrol.2009.08.003

Hague, B. S., & Taylor, A. J. (2021). Tide-only inundation: A metric to quantify the contribution of tides to coastal inundation under sea-level rise. *Natural Hazards*, *107*(1), 675–695. https://doi.org/10.1007/s11069-021-04600-4

Hino, M., Belanger, S. T., Field, C. B., Davies, A. R., & Mach, K. J. (2019). High-tide flooding disrupts local economic activity. *Science Advances*, *5*(2), eaau2736. https://doi.org/10.1126/sciadv.aau2736

Kalnay, E., Kanamitsu, M., Kistler, R., Collins, W., Deaven, D., Gandin, L., et al. (1996). The NCEP/NCAR 40-year reanalysis project. *Bulletin of the American Meteorological Society*, *77*(3), 437–471. https://doi.org/10.1175/1520-0477(1996)077<0437:TNYRP>2.0.CO;2

Kerns, B. W., & Chen, S. S. (2023). Compound effects of rain, storm surge, and river discharge on coastal flooding during Hurricane Irene and Tropical Storm Lee (2011) in the Mid-Atlantic region: Coupled atmosphere-wave-ocean model simulation and observations. *Natural Hazards*, *116*(1), 693–726. https://doi.org/10.1007/s11069-022-05694-0

Lee, S. B., Li, M., & Zhang, F. (2017). Impact of sea level rise on tidal range in Chesapeake and Delaware Bays. *Journal of Geophysical Research: Oceans*, *122*(5), 3917–3938. https://doi.org/10.1002/2016JC012597

Li, S., Wahl, T., Barroso, A., Coats, S., Dangendorf, S., Piecuch, C., et al. (2022). Contributions of different sea-level processes to high-tide flooding along the U.S. Coastline. *Journal of Geophysical Research: Oceans*, *127*(7). https://doi.org/10.1029/2021JC018276

Li, S., Wahl, T., Piecuch, C., Dangendorf, S., Thompson, P., Enríquez, A., & Liu, L. (2023). Compounding of sea-level processes during high-tide flooding along the U.S. Coastline. *Journal of Geophysical Research: Oceans*, *128*(8), e2023JC019885. https://doi.org/10.1029/2023JC019885

Li, S., Wahl, T., Talke, S. A., Jay, D. A., Orton, P. M., Liang, X., et al. (2021). Evolving tides aggravate nuisance flooding along the U.S. coastline. *Science Advances*, *7*(10), eabe2412. https://doi.org/10.1126/sciadv.abe2412

Mahmoudi, S., Moftakhari, H., Muñoz, D. F., Sweet, W., & Moradkhani, H. (2024). Establishing flood thresholds for sea level rise impact communication. *Nature Communications*, *15*(1), 4251. https://doi.org/10.1038/s41467-024-48545-1

Meade, R. H., & Emery, K. O. (1971). Sea level as affected by river runoff, eastern United States. *Science*, *173*(3995), 425–428. https://doi.org/10.1126/science.173.3995.425

Moftakhari, H. R., AghaKouchak, A., Sanders, B. F., Allaire, M., & Matthew, R. A. (2018). What is nuisance flooding? Defining and monitoring an emerging challenge. *Water Resources Research*, *54*(7), 4218–4227. https://doi.org/10.1029/2018WR022828

Moftakhari, H. R., AghaKouchak, A., Sanders, B. F., & Matthew, R. A. (2017a). Cumulative hazard: The case of nuisance flooding. *Earth's Future*, *5*(2), 214–223. https://doi.org/10.1002/2016EF000494

Moftakhari, H. R., Salvadori, G., AghaKouchak, A., Sanders, B. F., & Matthew, R. A. (2017b). Compounding effects of sea level rise and fluvial flooding. *Proceedings of the National Academy of Sciences*, *114*(37), 9785–9790. https://doi.org/10.1073/pnas.1620325114

Muñoz, D. F., Abbaszadeh, P., Moftakhari, H., & Moradkhani, H. (2022). Accounting for uncertainties in compound flood hazard assessment: The value of data assimilation. *Coastal Engineering*, *171*, 104057. https://doi.org/10.1016/j.coastaleng.2021.104057

Najjar, R., Patterson, L., & Graham, S. (2009). Climate simulations of major estuarine watersheds in the Mid-Atlantic region of the US. *Climatic Change*, *95*(1–2), 139–168. https://doi.org/10.1007/s10584-008-9521-y

Orton, P. M., Conticello, F. R., Cioffi, F., Hall, T. M., Georgas, N., Lall, U., et al. (2020). Flood hazard assessment from storm tides, rain and sea level rise for a tidal river estuary. *Natural Hazards*, *102*(2), 729–757. https://doi.org/10.1007/s11069-018-3251-x

Pareja-Roman, L. F., Chant, R. J., & Sommerfield, C. K. (2020). Impact of historical channel deepening on tidal hydraulics in the Delaware estuary. *Journal of Geophysical Research: Oceans*, *125*(12). https://doi.org/10.1029/2020JC016256

Pareja-Roman, L. F., Orton, P. M., & Talke, S. A. (2023). Effect of estuary urbanization on tidal dynamics and high tide flooding in a coastal lagoon. *Journal of Geophysical Research: Oceans*, *128*(1). https://doi.org/10.1029/2022JC018777

Partnership for the Delaware Estuary. (2022a). Five year strategic plan. *Partnership for the Delaware Estuary*. Retrieved from https://delawareestuary.org/about-pde/strategic-plan/

Partnership for the Delaware Estuary. (2022b). Technical report for the Delaware estuary and basin. In L. Haaf, L. Morgan, & D. Kreeger (Eds.), *PDE report No. 22-05* (p. 445). Retrieved from https://delawareestuary.org/data-and-reports/treb/

Piecuch, C. G. (2023). River effects on sea-level rise in the Río de la Plata estuary during the past century. *Ocean Science*, *19*(1), 57–75. https://doi.org/10.5194/os-19-57-2023

Piecuch, C. G., Bittermann, K., Kemp, A. C., Ponte, R. M., Little, C. M., Engelhart, S. E., & Lentz, S. J. (2018). River-discharge effects on United States Atlantic and Gulf coast sea-level changes. *Proceedings of the National Academy of Sciences*, *115*(30), 7729–7734. https://doi.org/10.1073/pnas.1805428115

Piecuch, C. G., Coats, S., Dangendorf, S., Landerer, F. W., Reager, J. T., Thompson, P. R., & Wahl, T. (2022). High-tide floods and storm surges during atmospheric rivers on the US west coast. *Geophysical Research Letters*, *49*(2). https://doi.org/10.1029/2021GL096820

Ralston, D. K., Talke, S., Geyer, W. R., Al-Zubaidi, H. A. M., & Sommerfield, C. K. (2019). Bigger tides, less flooding: Effects of dredging on barotropic dynamics in a highly modified estuary. *Journal of Geophysical Research: Oceans*, *124*(1), 196–211. https://doi.org/10.1029/2018JC014313

Ray, R. D., & Foster, G. (2016). Future nuisance flooding at Boston caused by astronomical tides alone: Tidal flooding. *Earth's Future*, *4*(12), 578–587. https://doi.org/10.1002/2016EF000423

Schober, P., Boer, C., & Schwarte, L. A. (2018). Correlation coefficients: Appropriate use and interpretation. *Anesthesia and Analgesia*, *126*(5), 1763–1768. https://doi.org/10.1213/ANE.0000000000002864

Serafin, K. A., Ruggiero, P., Parker, K., & Hill, D. F. (2019). What's streamflow got to do with it? A probabilistic simulation of the competing oceanographic and fluvial processes driving extreme along-river water levels. *Natural Hazards and Earth System Sciences*, *19*(7), 1415–1431. https://doi.org/10.5194/nhess-19-1415-2019

Sharp, J. (1984). Delaware Estuary: Research as background for estuarine management and development. In *Delaware River and bay authority rep. DEL-SG-03-84* (p. 340). University of Delaware Sea Grant College Program.

Sweet, W. V., Hamlington, B. D., Kopp, R. E., Weaver, C. P., Barnard, P. L., Bekaert, D., et al. (2022). *Global and regional Sea Level rise scenarios for the United States: Updated mean projections and extreme water level probabilities along U.S. Coastlines*. NOAA Technical Report NOS 01. National Oceanic and Atmospheric Administration, National Ocean Service. Retrieved from https://oceanservice.noaa.gov/hazards/sealevelrise/noaa-nostechrpt01-global-regional-SLR-scenarios-US.pdf

Sweet, W. V., Simon, S., Dusek, G., Marcy, D., Brooks, W., Pendleton, M., & Marra, J. (2021). *2021 state of high tide flooding and annual Outlook*. National Oceanic and Atmospheric Administration, National Ocean Service. https://doi.org/10.25923/MX62-RX21

Talke, S. A., & Jay, D. A. (2020). Changing tides: The role of natural and anthropogenic factors. *Annual Review of Marine Science*, *12*(1), 121–151. https://doi.org/10.1146/annurev-marine-010419-010727

Talke, S. A., Mahedy, A., Jay, D. A., Lau, P., Hilley, C., & Hudson, A. (2020). Sea level, tidal, and river flow trends in the lower columbia River Estuary, 1853–present. *Journal of Geophysical Research: Oceans*, *125*(3). https://doi.org/10.1029/2019JC015656

Thompson, P. R., Widlansky, M. J., Hamlington, B. D., Merrifield, M. A., Marra, J. J., Mitchum, G. T., & Sweet, W. (2021). Rapid increases and extreme months in projections of United States high-tide flooding. *Nature Climate Change*, *11*(7), 584–590. https://doi.org/10.1038/s41558-021-01077-8

USACE, P. D. (2022). *Delaware river main channel deepening*. US Army Corps of Engineers. Retrieved from https://www.nap.usace.army.mil/Missions/Factsheets/Fact-Sheet-Article-View/Article/490804/delaware-river-main-channel-deepening/

USACE, P. D. (2023). *Army Corps awards contract for Delaware River maintenance dredging*. US Army Corps of Engineers. Retrieved from https://www.nap.usace.army.mil/Media/News-Releases/Article/3446298/army-corps-awards-contract-for-delaware-river-maintenance-dredging/

Van Rijn, L. C. (2011). Analytical and numerical analysis of tides and salinities in estuaries; part I: Tidal wave propagation in convergent estuaries. *Ocean Dynamics*, *61*(11), 1719–1741. https://doi.org/10.1007/s10236-011-0453-0

Wahl, T., Jain, S., Bender, J., Meyers, S. D., & Luther, M. E. (2015). Increasing risk of compound flooding from storm surge and rainfall for major US cities. *Nature Climate Change*, *5*(12), 1093–1097. https://doi.org/10.1038/nclimate2736

Ward, P. J., Couasnon, A., Eilander, D., Haigh, I. D., Hendry, A., Muis, S., et al. (2018). Dependence between high sea-level and high river discharge increases flood hazard in global deltas and estuaries. *Environmental Research Letters*, *13*(8), 084012. https://doi.org/10.1088/1748-9326/aad400

Whitney, M. M., & Garvine, R. W. (2006). Simulating the Delaware bay buoyant outflow: Comparison with observations. *Journal of Physical Oceanography*, *36*(1), 3–21. https://doi.org/10.1175/JPO2805.1

Williamson, T. N., Nystrom, E. A., & Milly, P. C. D. (2016). Sensitivity of the projected hydroclimatic environment of the Delaware River basin to formulation of potential evapotranspiration. *Climatic Change*, *139*(2), 215–228. https://doi.org/10.1007/s10584-016-1782-2

Woltemade, C. J., Hawkins, T. W., Jantz, C., & Drzyzga, S. (2020). Impact of changing climate and land cover on flood magnitudes in the Delaware River Basin, USA. *JAWRA Journal of the American Water Resources Association*, *56*(3), 507–527. https://doi.org/10.1111/1752-1688.12835

Ye, F., Zhang, Y. J., Yu, H., Sun, W., Moghimi, S., Myers, E., et al. (2020). Simulating storm surge and compound flooding events with a creek-to-ocean model: Importance of baroclinic effects. *Ocean Modelling*, *145*, 101526. https://doi.org/10.1016/j.ocemod.2019.101526